Population Pharmacokinetic Analysis of Dexmedetomidine in Children using Real World Data from Electronic Health Records and Remnant Specimens

Nathan T. James[1], Joseph H. Breeyear[2], Richard Caprioli[2], Todd Edwards[2], Brian Hachey[2], Prince J. Kannankeril[3,5], Jacob M. Keaton[2,6], Matthew D. Marshall[4], Sara L. Van Driest[2,3,5], Leena Choi[1]

Departments of [1]Biostatistics, [2]Medicine, [3]Pediatrics and [4]Pharmaceutical Services and [5]Center for Pediatric Precision Medicine, Vanderbilt University Medical Center, Nashville, TN; [6]Center for Precision Health Research, National Human Genome Research Institute, National Institutes of Health, Bethesda, MD.

Corresponding Author: Dr. Leena Choi, PhD, Department of Biostatistics, Vanderbilt University Medical Center, Nashville, TN, USA. Tel: +1 615 343 3497; Fax: +1 615 343 4924; E-mail: leena.choi@vumc.org

Principal Investigator Statement: The authors confirm that the PIs for this paper are Leena Choi and Prince J. Kannankeril.

Running Head: Dexmedetomidine Population Pharmacokinetics

Key Words: Population Pharmacokinetics, Dexmedetomidine, Pragmatic Research, Opportunistic Sampling, Real-World Data

Word Count: 4077

Table Count: 2

Figure Count: 3

What is already known about this subject

- Previous dexmedetomidine pharmacokinetic (PK) studies in pediatric populations have limited sample size.
- Smaller studies present a challenge for identifying covariates that may impact individual PK profiles.

What this study adds

- We performed a dexmedetomidine population PK study with a large pediatric cohort using data obtained from electronic health records and remnant plasma specimens to enable increased sample size.
- Differences in PK due to *UGT1A4* or *UGT2B10* variants or *CYP2A6* risk score are not clinically impactful for this population.

Abstract

Aim

Our objectives were to perform a population pharmacokinetic analysis of dexmedetomidine in children using remnant specimens and data from electronic health records (EHRs) and explore the impact of patient's characteristics and pharmacogenetics on dexmedetomidine clearance.

Methods

Dexmedetomidine dosing and patient data were gathered from EHRs and combined with opportunistically sampled remnant specimens. Population pharmacokinetic models were developed using nonlinear mixed-effects modeling. The first stage developed a model without genotype variables; the second stage added pharmacogenetic effects.

Results

Our final study population included 354 post-cardiac surgery patients age 0 to 22 years (median 16 months). The final two-compartment model included allometric weight scaling and age maturation. Population parameter estimates and 95% confidence intervals were 27.3 L/hr (24.0 – 31.1 L/hr) for total clearance (CL), 161 L (139 – 187 L) for central compartment volume of distribution (V_1), 26.0 L/hr (22.5 – 30.0 L/hr) for intercompartmental clearance (Q), and 7903 L (5617 – 11119 L) for peripheral compartment volume of distribution (V_2). The estimate for postmenstrual age when 50% of adult clearance is achieved was 42.0 weeks (41.5 – 42.5 weeks) and the Hill coefficient estimate was 7.04 (6.99 – 7.08). Genotype was not statistically or clinically significant.

Conclusion

Our study demonstrates the use of real-world EHR data and remnant specimens to perform a population PK analysis and investigate covariate effects in a large pediatric population. Weight and age were important predictors of clearance. We did not find evidence for pharmacogenetic effects of *UGT1A4* or *UGT2B10* genotype or *CYP2A6* risk score.

Introduction

Dexmedetomidine is an alpha2-agonist with anxiolytic, sedative, and analgesic properties with minimal effects on respiratory depression.[1,2] It is routinely used as part of intraoperative anesthetic management during surgical repairs of congenital heart disease (CHD) and in the postoperative period in the intensive care unit (ICU)[3,4] and is commonly dosed as a continuous intravenous (IV) infusion using a fixed weight-based rate (e.g., starting at 0.3 mcg/kg/h). This dosing regimen will be adequate for some, but necessarily results in inappropriately low or high

dosing for others. The proper dose for these latter individuals is not achieved until the initial sedation effect is observed, recognized as inadequate or excessive by the clinical team, and the dose adjusted accordingly. These patients are at risk for dose-related dexmedetomidine side effects, including bradycardia and hypotension, or use of additional sedative agents, including opioid analgesics. Accurate prediction of an individual's dexmedetomidine requirement (precision dosing) could help minimize titration time to achieve sedation and analgesia goals without toxicity.

Many population pharmacokinetic (PK) studies of dexmedetomidine in pediatric populations have been reported.[5–17] For example, Potts et al.[17] report on dexmedetomidine use in 95 pediatric ICU patients using data pooled from several previous studies, Su et al.[15] studied 59 children on mechanical ventilation after open heart surgery, Pérez-Guillé et al.[12] assessed 30 children undergoing ambulatory surgery, and Zuppa et al.[9] examined dexmedetomidine PK among 119 children undergoing cardiac surgery. Most have a small number of individuals and frequent specimen collection. For pediatric ICU populations, the median sample size is 29.5 (range 18-119), and the median number of total drug levels collected is 236.5 (range 89 – 1967) with a median of 9 per subject (range 2 – 16).[5,7,9–12,14,15] Some studies have addressed small sample size with methods that combine information from multiple populations including pooled pediatric analyses,[17] creating "universal" models for children and adults,[6,8] and Bayesian analyses with informative priors;[16] however, even these models only include information from at most around 130 children.

Previously, studies have identified weight[5–12,14–17] and age[5,6,8–10,14–17], along with cardiac bypass[9,10,15], as important factors to explain inter-individual variability. However, lower sample size may limit identification of additional covariates impacting inter-individual variability. For example, although it is known that dexmedetomidine is rapidly distributed and metabolized in the liver by two pathways – direct glucuronidation by uridine 5′-diphosphate-

glucuronosyltransferase (UGT) 1A4 and 2B10 and cytochrome P450 (CYP) 2A6 mediated aliphatic hydroxylation[2,18] – small studies of the impact of genetic variation or expression levels of these enzymes have failed to demonstrate pharmacogenetic associations.[19,20] A study including 260 children demonstrated that carriers of the T allele of *CYP2A6* rs835309 had significantly lower concentrations of dexmedetomidine (TT + TG vs. GG, p – value = .025).[21] A newly developed weighted genetic risk score to predict *CYP2A6* activity raises the possibility of better capturing the impact of variants across this gene for pharmacogenetic analysis.[22] Study of a larger cohort may allow the identification of genetic biomarkers affecting dexmedetomidine PK, facilitating precision dosing based on genotype.

We combined data from electronic health records (EHRs) and remnant specimens collected during usual clinical care to perform a population PK analysis, similar to two previous pediatric fentanyl studies, and employing a system for constructing PK analysis datasets in R.[23–26] The major goals of this study were to develop a dexmedetomidine population PK model for children with data obtained from EHRs and remnant specimens and quantify genetic effects that were selected *a priori* based on previous studies and known metabolic pathways.

Methods

Study Design

This study was approved by the Vanderbilt University Medical Center (VUMC) Institutional Review Board and has been previously described.[23] In brief, pediatric patients undergoing surgery for CHD are offered enrollment in this observational study. Parents provide written consent for their child's participation, and informed assent is obtained when appropriate. Drug selection and dosing are determined by the primary clinical team; over the course of study enrollment, clinical leadership provided recommended protocols to guide clinicians in drug and

dose selection for analgesia and sedation (included in supplemental material); however, final regimens were always at the discretion of the treating clinicians. Remnant specimens from clinical testing are obtained for drug concentration measurements, which are not disclosed to the clinical teams. Specimens were not collected in connection with dose administration or to monitor PK characteristics such as trough concentration or C_{max}. Enrollment with remnant specimen collection began in July 2012 and is ongoing. Data analyzed for this study were collected prior to October 2017. All study participants were admitted to the pediatric cardiac ICU after surgery. Enrolled participants were excluded from the analysis if their surgery was cancelled, if there was missing genotype data, if extracorporeal membrane oxygenation (ECMO) treatment was required, or if they did not survive to hospital discharge. For those with multiple surgeries, data from the one procedure with the highest number of measured serum drug concentrations were used, excluding all others. Drug concentrations were excluded if inadequate internal standard concentrations were detected and insufficient volume remained to repeat analysis, or if they were obtained before any documented dexmedetomidine dosing.

Data Collection

Demographic data (including parent-reported race) and medical history were documented at the time of study enrollment. Surgical and clinical data were extracted from the EHR prospectively. Dexmedetomidine dosing, including scheduled boluses, as-needed intermittent boluses, and continuous infusions after the postoperative admission to the ICU were determined from the EHR and the Vanderbilt Enterprise Data Warehouse. The Enterprise Data Warehouse contains nurse administration, nurse flowsheets, and pharmacy dispense data, enabling the computation of administered drug amounts over specific time periods. Study data were collected and managed

using REDCap electronic data capture tools, a secure, web-based application hosted at Vanderbilt University.[27]

Drug Concentration Measurement

For the purposes of drug concentration analysis, all remnant plasma specimens ≥100 μL from blood obtained for clinical testing of electrolyte or basic metabolic panels in study subjects were obtained from the Vanderbilt Clinical Chemistry Laboratory and stored at -20ºC until processing for drug concentration analysis in the Vanderbilt Mass Spectrometry Research Core. Specimen processing and mass spectrometry analysis have been previously described in detail.[23] Briefly, acetonitrile precipitation was followed by tandem mass spectrometry using a 16-drug assay. Dexmedetomidine assay accuracy is 89 – 112%, and the lower and upper limits of quantification (LLOQ and ULOQ) are 0.005 and 5 ng/mL.

Genotyping and CYP2A6 Activity Score Prediction

Study participants provided a peripheral blood sample for genetic analysis. Genomic DNA was extracted through the Vanderbilt Technologies for Advanced Genomics (VANTAGE) Core laboratory and study participants were genotyped using either the Axiom™ Precision Medicine Research Array or the Precision Medicine Diversity Array according to manufacturer protocols at the Children's Hospital of Philadelphia DNA core. As part of genotype data quality control, variants were removed if genotype call rate was <98%, if minor allele frequency was >20% different from 1000 Genomes phase 3 European reference populations, or for deviation from Hardy-Weinberg Equilibrium (p – value < $1x10^{-10}$, results shown in **Supplemental Table S3**). Individuals were removed if their genotype call rate was <98%, the genetically estimated sex

differed from parental-reported sex, or for relatedness (2nd degree or closer). Genotype data were imputed to the 1000 Genomes phase 3 reference panel. For this study, we extracted data for specific variants in *UGT2B10* (rs2942857; rs112561475; rs61750900), *UGT1A4* (rs2011425; rs3892221; rs6755571) and *CYP2A6* (rs56113850; rs2316204; rs113288603; rs28399442; rs1801272; rs28399433) from the study database.

Data Processing

Data was processed using the modularized "*EHRtoPKPD*" system for postmarketing population PK studies with real-world data from EHRs.[25] This system has been implemented in the R software[28] package EHR[26] which includes interactive checks for data quality to reconcile missing, duplicate, and other erroneous concentration or dosing information (for details, see https://choileena.github.io/). Output from the EHR package was further cleaned by removing: (i) concentration measurements more than 150 hrs (approximately 50 times dexmedetomidine half-life) after the end of the final bolus or infusion dose, (ii) concentration measurements below the LLOQ if they are after the final bolus or infusion dose, except for the first such measurement, (iii) concentration measurements above the ULOQ, (iv) subjects whose only concentration measurements are below the LLOQ after applying criteria (i)-(iii), and (v) subjects with missing dose information indicated by increases in concentration without an accompanying dose and confirmed by manual chart review.

Serum creatinine concentration was a time-varying covariate typically measured concurrently with dexmedetomidine concentration. If serum creatinine was not available when dexmedetomidine concentration was measured, we selected the serum creatinine concentration measured closest to the dexmedetomidine concentration data within 7 days. For each subject, weight varied little within the timeframe of available concentration data, so most weight data

were the same as the baseline demographic measurements. When additional weight measurements were available, usually during infusion, weight measurements obtained at the same time as the dosing event were used. Measures of albumin concentration were available within a 7-day window for only 48 subjects, precluding use of albumin concentration as a covariate.

Population PK Analysis

We performed population PK analysis of dexmedetomidine using nonlinear mixed-effects models implemented by Monolix version 2020R1[29] and estimated the parameters with the stochastic approximation expectation-maximization (SAEM) algorithm. Observed concentrations below the LLOQ were considered to be censored between 0 and 0.005 ng/mL and were handled in the modeling using the likelihood (M3) method for interval censoring.[30,31] After the model parameters were estimated with SAEM, the objective function value (OFV) was calculated using Monte Carlo importance sampling with 10,000 samples from a Student-t proposal distribution and degrees of freedom chosen by testing a sequence of values (ν =1, 2, 5, 10, 15). Because the SAEM estimation method includes stochastic variability and can sometimes fail to converge in a setting with sparse sampling,[32] we performed 5 runs with different random seeds for each model and selected the run with median OFV for model comparison.

For model selection we used a likelihood ratio test to compare differences in estimated OFV for nested models and corrected Bayesian Information Criteria (BICc) to compare non-nested models; relative standard errors, parameter estimate values, magnitude of random effects and change in CV% were also considered. In addition, we used several graphical methods for model evaluation including observed vs. population and individual predictions, individual weighted residuals vs. predicted concentration and time, correlations between samples from the

conditional random effects distributions, samples from the conditional random effects distributions vs. covariates, and prediction corrected visual predictive checks.[33,34]

All covariates were chosen *a priori* based on previous research and biological plausibility, including *UGT1A4*, *UGT2B10*, and *CYP2A6* variants, age, sex, Society of Thoracic Surgery–European Association for Cardio-Thoracic Surgery (STAT) Congenital Heart Surgery Mortality score,[35] cardiac bypass time, length of ICU stay, and serum creatinine. We focused on modeling the effects of covariates on total clearance, although the graphical checks were examined for possible relationships between covariates and other PK parameters.

Model building proceeded in two stages; we first considered all covariates except *UGT1A4*, *UGT2B10*, and *CYP2A6* to build an adequate model for dexmedetomidine PK and then examined the hypothesized association between the genotype variables and total clearance by adding these effects individually to the stage one model. For stage one we explored models with various structural, residual error, and inter-individual variance components and adjusted for non-genotype covariates. Following a strategy outlined by Bonate, we began with richly parameterized inter-individual variability and residual error models including all random effects, all correlations between random effects, and combined additive and proportional residual error, and then simplified this structure.[36] We examined the structural model by comparing one- and two-compartment models without covariates. Following this we considered size and age maturation; these two covariates have been shown to be important factors in pediatric PK models with a large age range and in previous dexmedetomidine studies.[6,8,16,17,37–39] For size, we employed an allometric weight model with fixed or estimated scaling parameters. For maturation, we considered an exponential age model, a sigmoid Hill maturation model, a body-weight dependent exponent model, and an age-dependent exponent model.[40] Next, we investigated whether other non-genotype covariates improved the model with size and

maturation factors and refined residual and inter-individual variance structure. Each covariate was considered as an exponentially linear or categorical term.

In the second stage we tested for the association between genotype and total clearance by including these effects in the model found in stage one. For *UGT1A4* and *UGT2B10*, dichotomous models (coding individuals as having a loss-of-function variant or not) and additive models (counting the number of variants) were considered. For *CYP2A6*, enzyme activity was predicted using a polygenic score and included as an exponential term.[22] Details of all models explored along with specific mathematical relationships, estimated OFV, and BICc are shown in **Supplemental Tables S3 – S10**. Graphical checks for the model selection process are shown in **Supplemental Figures S3 – S27**.

Results

Study Population and Specimens

We collected 4,369 residual plasma specimens from 620 subjects. After removing 89 subjects with unknown sample collection time, 108 subjects with no dosing information within 7 days of the first concentration measurement, and 14 subjects due to in hospital mortality or ECMO, the output of the EHR package pipeline contained 411 subjects with 2,172 dexmedetomidine concentration measurements. The further cleaning steps described above removed 14 subjects and 43 more subjects without genotype information were also removed. The study cohort flow diagram of data processing is shown in **Figure 1,** and the final study population of 354 subjects with 1,400 specimens is described in **Table 1**. The median postnatal age was 16 months (interquartile range [IQR] 5 – 62), median postmenstrual age was 105 weeks (IQR 62 - 304) and median weight was 9.4 kg (IQR 6.0 – 18.2). The age and weight distributions are shown in **Supplemental Figures S1** and **S2** and **Supplemental Table S1** shows postnatal age categories.

There were 262 subjects (74%) with no variants of *UGT1A4*, 87 (25%) with 1 variant and 5 (1%) with 2 variants. For *UGT2B10*, 186 subjects (53%) had no variants, 117 (33%) had 1 variant and 51 (14%) had 2 or 3 variants. The *CYP2A6* predicted activity score was available for 350 of the 354 subjects (median 2.04, IQR 2.00 – 2.21). There were 2,386 dexmedetomidine dosing events (2,351 IV infusions and 35 bolus administrations). The median infusion rate was 0.6 mcg/kg/hr (IQR 0.5 – 1.0) and the median infusion duration was 2 hours (IQR 1 - 5); the median bolus dose was 1.0 mcg/kg (IQR 0.96 – 1.01). The top ten concomitant medications were acetaminophen (92.5%), cefazolin (92%), famotidine (89.1%), morphine (88.5%), furosemide (80.5%), fentanyl (77.9%), rocuronium (69.5%), oxycodone (59.8%), heparin (58.3%), and lorazepam (51.4%). **Supplemental Table S2** includes all concomitant medications administered to at least 5% of subjects. The number of dexmedetomidine concentration measurements per subject varied from a minimum of 1 to a maximum of 18 with a median of 3 specimens (IQR 2 – 5). The median time of first dexmedetomidine measurement after dose start was 5 hours (IQR 4 – 11) and the median time of final dexmedetomidine measurement after dose start was 68 hours (IQR 39 – 131).

Population PK Model

In the first stage of modeling, a two-compartment model with additive and proportional residual error was chosen as the base model based on BICc and graphical checks. The main PK parameters are total clearance (CL, L/h), volume of distribution for the central compartment (V_1, L), inter-compartmental clearance (Q, L/h) and volume of distribution for the peripheral compartment (V_2, L). The results for the base and covariate models without genotype are presented in **Table 2A**. The coefficients of variation (CV) for CL, V_1, Q, and V_2 in the base model were 201%, 161%, 146%, and 672%, respectively.

Including weight as covariate for all PK parameters with fixed allometric scaling parameters substantially improved the model fit (both OFV and BICc decreased by 406 from the base model, **Table 2A**) and plots of individual predicted vs. observed concentration, individual weighted residuals vs. predicted concentration and random effects vs. covariates also improved (**Supplemental Figures S8 – S12**). The CV for CL, V_1, Q, and V_2 were 123%, 168%, 91%, and 857%, respectively. Using estimated allometric parameters did not improve the model fit.

Among the four models adjusting for both weight and age maturation, the model with sigmoid postmenstrual age maturation had the largest improvement in BICc compared to the model with only weight (difference of 8.2, **Table S5**). This model was further simplified by estimating models with fixed effects for V_2 or V_2 and Q, no additive residual error component, and several correlation structures for the covariance between random effects (**Table S6**). The final model without genetic effects includes proportional residual error, fixed allometric scaling for all parameters and sigmoid (Hill) maturation for total clearance, random effects for all PK parameters and correlation only between the random effects of CL and V_1 (**Table 2A**). No further improvement was seen by adding other covariates including either form of *UGT1A4* or *UGT2B10* or predicted *CYP2A6* activity score (Tables **2B**, **2C**, and **2D**) and no strong covariate effects were seen for V_1, Q, or V_2 based on graphical goodness-of-fit plots. The final covariate model is described as follows:

$$CL_i = \theta_1 \times (WT_i/70)^{0.75} \times 1/1+(TM_{50}/PMA_i)^{Hill} \times \exp(\eta_i^{CL})$$

$$V_{1i} = \theta_2 \times (WT_i/70) \times \exp(\eta_i^{V1})$$

$$Q_i = \theta_3 \times (WT_i/70)^{0.75} \times \exp(\eta_i^{Q})$$

$$V_{2i} = \theta_4 \times (WT_i/70) \times \exp(\eta_i^{V2}),$$

where CL_i, V_{1i}, Q_i, and V_{2i} are the individual-specific PK parameters corresponding to CL, V_1, Q, and V_2, WT_i is subject weight in kilograms (kg), and PMA_i is subject postmenstrual age in

weeks. The η_i^{CL}, $\eta_i^{V_1}$, η_i^{Q}, and $\eta_i^{V_2}$ are random effects explaining inter-individual variability for the PK parameters which follow a normal distribution with mean zero and variance of ω^2_{CL}, ω^2_{V1}, ω^2_{Q}, and ω^2_{V2}, respectively. The θs are estimated model parameters. Diagnostic plots for the final model are shown in **Figure 2**. The plot of observed dexmedetomidine concentrations vs. population predictions reflects the relatively large inter-individual variability and potential misspecification for small concentration values, however no major deficiencies in the structural or error models are seen when comparing observed and individual predicted concentrations. No trends were detected in plots of individual weighted residuals vs. predicted concentration or time. The prediction-corrected visual predictive check showed good agreement between the observed and theoretical median and 90th percentiles; model misspecification is seen for the 10th percentile where many values are below the LLOQ and were simulated from the estimated model and where data are sparse (e.g., times greater than 5 days after first dose).

The estimates of CL, V_1, Q and V_2 in terms of a standard weight of 70 kg are shown in **Table 2A**: CL (θ_1) = 27.3 L/h, V_1 (θ_2) = 161 L, Q (θ_3) = 26.0 L/h, and V_2 (θ_4) = 7903 L. We estimate CL, V_1, Q and V_2 as 6.04 L/h, 21.6 L, 5.7 L/h, and 1061.26 L for a child at the median weight of 9.4 kg and median postmenstrual age of 104.6 weeks; After including covariates, the CV for CL was substantially reduced from 201% estimated in the base model to 123% in the weight only model to 103% in the final model. CV remains large for some parameters, especially V_2 (624%) and V_1 (138%), indicating that we lack the data to estimate them with precision.

Model estimated clearance from the final model for seven age groups across a range of plausible weights is shown in **Figure 3** (overlap between lines indicates weights that are plausible for multiple age groups). Weight impacts mean estimated CL for all ages while postmenstrual age has a large impact only for the youngest age groups. For those over 93 weeks

postmenstrual age, maturation is near adult level and mean estimated CL is primarily determined by weight.

Genetic Effects on Clearance and Concentration

UGT1A4, *UGT2B10*, and *CYP2A6* were not significant at the $\alpha = 0.05$ level. For the *UGT1A4* categorical gene model the estimated effect of any variants vs. no variants was -0.221 (95% CI: -0.54 to 0.09) for a 20% decrease [$\exp(-0.221) \approx 0.80$] in CL on average for those with any *UGT1A4* variants holding age and weight constant. In the *UGT1A4* additive gene model, the estimated effect of each additional variant was -0.166 (95% CI: -0.406 to 0.073). For the *UGT2B10* categorical model, the estimated genotype effect was -0.104 (95% CI: -0.32 to 0.11), indicating a 10% decrease on average. The *UGT2B10* additive model estimated the effect of additional variants as -0.108 (95% CI: -0.241 to 0.025). For the *CYP2A6* model, the estimated effect of a unit increase in risk score was 0.0885 (95% CI: -0.46 to 0.64).

Although these effects are not statistically significant using the $\alpha = 0.05$ threshold, we perform simulations to assess the hypothetical impact on total clearance and clinical dosing if the categorical *UGT1A4* or *UGT2B10* model estimates were utilized. Results are included in **Supplemental Figures S29 – S34**. Including these effects in the PK model has a negligible impact on dosing.

Discussion

Using remnant specimens along with dosing, clinical, and demographic information from an EHR system we were able to develop a dexmedetomidine population PK model for a large

pediatric cohort of 354 patients. We identified patient characteristics that alter the PK profile. This study is one of the largest pediatric dexmedetomidine population PK studies reported.

We confirmed a structural model and covariate relationships which are in line with those previously reported for dexmedetomidine PK. Specifically, our model included both weight and age maturation effects on CL. We estimated a weight-standardized CL of 27.3 L/h (CV 103%). Our estimated CL is somewhat smaller (with larger CV) than those reported in other pediatric PK studies. For a standard weight of 70 kg, Potts et al.[17] found a population CL estimate of 42.1 L/h (CV 30.9%); including a scaling factor of 0.73 for children given infusion (vs. bolus) reduced the CL estimate to 30.7 L/h. Zuppa et al.[9] estimated CL of 37.3 L/h (CV 48%) for neonates and infants age 0 – 6 months after cardiac bypass and Su et al.[15] estimated CL as 39.4 L/h (CV 28%) for children age 1 – 24 months after open heart surgery. The discrepancy between studies could be related to several factors including study design and study population. For example, our study used sparse and opportunistic sampling and included a more heterogenous population which included older children while the other studies used densely measured drug levels and were performed in a well-controlled clinical setting with a younger and more homogeneous population. After controlling for weight and age maturation, we found little evidence to support the importance of UGT1A4, UGT2B10, or CYP2A6 effects in explaining variability of CL between subjects.

Using population PK models derived from EHR data and remnant specimens offers the possibility of more accurate prediction of individual dosing requirements in a real-life setting, especially in populations where large, intensive-sampling PK clinical trials are difficult to perform due to ethical or logistical considerations. The results from such model-informed precision dosing could also be integrated into EHR-embedded decision support tools; the

development and implementation of several of these tools has been recently described by Mizuno et al.[41] and Vinks et al.[42]

There are several limitations related to the use of EHR and remnant specimens for our study. Although our data were generated using a standardized system to construct the PK data,[25] there may be some errors due to inherent limitations of EHR data, which is not primarily collected for research use. First, data collected for clinical purposes may be subject to errors related to data entry or missingness. Further, real-world dosing data are not standardized with large heterogeneity in the frequency, duration, and timing of administered infusion and bolus doses. In addition, the specimens are very sparse for some subjects and their collection is not timed to facilitate optimal PK estimation. These limitations may be related to the imprecision in estimates for some PK parameters, notably V_2. Future studies could address some of these limitations by incorporating prior information from previous or smaller pilot studies with more densely sampled data.

Despite these limitations, our study provides further evidence for the feasibility of using EHR data and remnant specimens for population PK analysis. Our study findings, such as weight effects on CL, could be helpful to develop a model-based dosing that may be superior to the current fixed weight-based dosing scheme. However, this should be tested in a future study for its clinical utility in the pediatric population. Because dexmedetomidine is used to achieve specific sedation goals, it would also be of interest to incorporate the current study results into a joint pharmacokinetic-pharmacodynamic model using sedation outcomes also derived from the EHR. These models are an important step toward the ultimate goal of precision dosing.

Acknowledgements

The authors thank the Vanderbilt Clinical Laboratory staff for their assistance in obtaining the remnant specimens for this research, the patients and families who participated in this study, Ahmed Elboraie and Rachel Tyndale for assistance with the *CYP2A6* genetic risk score, and Cole Beck for assistance with the concomitant medications.

Conflict of Interest / Disclosure

None

Funding: LC, NTJ, and SLV are supported by NIH/NIGMS (R01 GM124109). This work was supported in part by NIH/NIGMS (MS), NICHD R01 HD084461 and NIH National Center for Advancing Translational Sciences UL1 TR000445 (Vanderbilt CTSA).

Author Contributions

All authors participated in critical review and revision of the final manuscript and approved the final manuscript draft.

NTJ: analyzed data, performed research, and wrote manuscript. JHB: analyzed data.
RC: designed research and contributed analytical tools. TE: performed research.
BH: designed research, performed research and contributed analytical tools. PJK: designed research and wrote manuscript. JK: performed research. MDM: extracted data and analyzed data.
SLV: designed research, performed research and wrote manuscript. LC: designed research, analyzed data, performed research, and wrote manuscript.

Data Availability Statement

The data that support the findings of this study are available from the corresponding author upon reasonable request.

References

1. Plambech, M. Z. & Afshari, A. Dexmedetomidine in the pediatric population: a review. *MINERVA Anestesiol.* **81**, 13 (2015).
2. Weerink, M. A. S. *et al.* Clinical Pharmacokinetics and Pharmacodynamics of Dexmedetomidine. *Clin. Pharmacokinet.* **56**, 893–913 (2017).
3. Schwartz, L. I. *et al.* The Perioperative Use of Dexmedetomidine in Pediatric Patients with Congenital Heart Disease: An Analysis from the Congenital Cardiac Anesthesia Society-Society of Thoracic Surgeons Congenital Heart Disease Database. *Anesth. Analg.* **123**, 715–721 (2016).
4. Shuplock, J. M. *et al.* Association between perioperative dexmedetomidine and arrhythmias after surgery for congenital heart disease. *Circ. Arrhythm. Electrophysiol.* **8**, 643–650 (2015).
5. Takeuchi, M. *et al.* Age-Specific Dose Regimens of Dexmedetomidine for Pediatric Patients in Intensive Care Following Elective Surgery: A Phase 3, Multicenter, Open-Label Clinical Trial in Japan. *Pediatr. Crit. Care Med.* (2021).doi:10.1097/PCC.0000000000002730
6. Morse, J. D., Cortinez, L. I. & Anderson, B. J. A Universal Pharmacokinetic Model for Dexmedetomidine in Children and Adults. *J. Clin. Med.* **9**, 3480 (2020).
7. Damian, M. A. *et al.* Pharmacokinetics of Dexmedetomidine in Infants and Children After Orthotopic Liver Transplantation: *Anesth. Analg.* **130**, 209–216 (2020).
8. Ber, J. *et al.* Population Pharmacokinetic Model of Dexmedetomidine in a Heterogeneous Group of Patients. *J. Clin. Pharmacol.* **60**, 1461–1473 (2020).
9. Zuppa, A. F. *et al.* Results of a phase 1 multicentre investigation of dexmedetomidine bolus and infusion in corrective infant cardiac surgery. *Br. J. Anaesth.* **123**, 839–852 (2019).
10. Zimmerman, K. O. *et al.* Dexmedetomidine Pharmacokinetics and a New Dosing Paradigm in Infants Supported With Cardiopulmonary Bypass: *Anesth. Analg.* **129**, 1519–1528 (2019).
11. Song, I.-K. *et al.* A Population Pharmacokinetic Model of Intravenous Dexmedetomidine for Mechanically Ventilated Children after Neurosurgery. *J. Clin. Med.* **8**, 1563 (2019).
12. Pérez-Guillé, M.-G. *et al.* Population Pharmacokinetics and Pharmacodynamics of Dexmedetomidine in Children Undergoing Ambulatory Surgery: *Anesth. Analg.* **127**, 716–723 (2018).
13. Smuszkiewicz, P. *et al.* Pharmacokinetics of dexmedetomidine during analgosedation in ICU patients. *J. Pharmacokinet. Pharmacodyn.* **45**, 277–284 (2018).

14. Greenberg, R. G. *et al.* Population Pharmacokinetics of Dexmedetomidine in Infants: Journal of Clinical Pharmacology. *J. Clin. Pharmacol.* **57**, 1174–1182 (2017).

15. Su, F. *et al.* Dexmedetomidine Pharmacology in Neonates and Infants After Open Heart Surgery: *Anesth. Analg.* **122**, 1556–1566 (2016).

16. Wiczling, P. *et al.* The pharmacokinetics of dexmedetomidine during long-term infusion in critically ill pediatric patients. A Bayesian approach with informative priors. *J. Pharmacokinet. Pharmacodyn.* **43**, 315–324 (2016).

17. Potts, A. L. *et al.* Dexmedetomidine pharmacokinetics in pediatric intensive care – a pooled analysis. *Pediatr. Anesth.* **19**, 1119–1129 (2009).

18. *DEXMEDETOMIDINE HCL injection [package insert]*. (Hikma Pharmaceuticals USA Inc., Berkeley Heights, NJ, 2020).at <https://dailymed.nlm.nih.gov/dailymed/drugInfo.cfm?setid=de6f01a2-9f2d-4c68-9c02-06643704acb1>

19. Kohli, U. *et al.* CYP2A6 genetic variation and dexmedetomidine disposition. *Eur. J. Clin. Pharmacol.* **68**, 937–942 (2012).

20. Rolle, A. *et al.* Dexmedetomidine metabolic clearance is not affected by fat mass in obese patients. *Br. J. Anaesth.* **120**, 969–977 (2018).

21. Guan, Y. *et al.* Quantitative ultra-high-performance liquid chromatography-tandem mass spectrometry for determination of dexmedetomidine in pediatric plasma samples: Correlation with genetic polymorphisms. *Biomed. Chromatogr. BMC* **33**, e4683 (2019).

22. El-Boraie, A. *et al.* Evaluation of a weighted genetic risk score for the prediction of biomarkers of CYP2A6 activity. *Addict. Biol.* **25**, e12741 (2020).

23. Van Driest, S. L. *et al.* Pragmatic pharmacology: population pharmacokinetic analysis of fentanyl using remnant samples from children after cardiac surgery. *Br. J. Clin. Pharmacol.* **81**, 1165–1174 (2016).

24. Hagos, F. T. *et al.* Factors Contributing to Fentanyl Pharmacokinetic Variability Among Diagnostically Diverse Critically Ill Children. *Clin. Pharmacokinet.* **58**, 1567–1576 (2019).

25. Choi, L. *et al.* Development of a System for Postmarketing Population Pharmacokinetic and Pharmacodynamic Studies Using Real-World Data From Electronic Health Records. *Clin. Pharmacol. Ther.* **107**, 934–943 (2020).

26. *EHR: Electronic Health Record (EHR) Data Processing and Analysis Tool*. (2020).at <https://cran.r-project.org/package=EHR>

27. Harris, P. A. *et al.* Research electronic data capture (REDCap)—A metadata-driven methodology and workflow process for providing translational research informatics support. *J. Biomed. Inform.* **42**, 377–381 (2009).

28. R Core Team *R: A Language and Environment for Statistical Computing*. (R Foundation for Statistical Computing, Vienna, Austria, 2020).at <https://www.R-project.org/>

29. *Monolix*. (Lixoft SAS, Antony, France, 2020).at <https://monolix.lixoft.com/>

30. Ahn, J. E., Karlsson, M. O., Dunne, A. & Ludden, T. M. Likelihood based approaches to handling data below the quantification limit using NONMEM VI. *J Pharmacokinet Pharmacodyn* 21 (2008).

31. Beal, S. L. Ways to Fit a PK Model with Some Data Below the Quantification Limit. *J. Pharmacokinet. Pharmacodyn.* **28**, 481–504 (2001).

32. Sukarnjanaset, W., Wattanavijitkul, T. & Jarurattanasirikul, S. Evaluation of FOCEI and SAEM Estimation Methods in Population Pharmacokinetic Analysis Using NONMEM® Across Rich, Medium, and Sparse Sampling Data. *Eur. J. Drug Metab. Pharmacokinet.* **43**, 729–736 (2018).

33. Lavielle, M. & Ribba, B. Enhanced Method for Diagnosing Pharmacometric Models: Random Sampling from Conditional Distributions. *Pharm. Res.* **33**, 2979–2988 (2016).

34. Nguyen, T. H. T. *et al.* Model Evaluation of Continuous Data Pharmacometric Models: Metrics and Graphics. *CPT Pharmacomet. Syst. Pharmacol.* **6**, 87–109 (2017).

35. Jacobs, M. L. *et al.* An empirically based tool for analyzing morbidity associated with operations for congenital heart disease. *J. Thorac. Cardiovasc. Surg.* **145**, 1046-1057.e1 (2013).

36. Bonate, P. L. *Pharmacokinetic-pharmacodynamic modeling and simulation*. (Springer, New York, 2011).

37. Anderson, B. J. & Holford, N. H. G. Tips and traps analyzing pediatric PK data. *Pediatr. Anesth.* **21**, 222–237 (2011).

38. Holford, N., Heo, Y.-A. & Anderson, B. A Pharmacokinetic Standard for Babies and Adults. *J. Pharm. Sci.* **102**, 2941–2952 (2013).

39. Back, H. *et al.* Application of Size and Maturation Functions to Population Pharmacokinetic Modeling of Pediatric Patients. *Pharmaceutics* **11**, 259 (2019).

40. Ding, J. *et al.* A Population Pharmacokinetic Model of Valproic Acid in Pediatric Patients with Epilepsy: A Non-Linear Pharmacokinetic Model Based on Protein-Binding Saturation. *Clin. Pharmacokinet.* **54**, 305–317 (2015).

41. Mizuno, T., Dong, M., Taylor, Z. L., Ramsey, L. B. & Vinks, A. A. Clinical implementation of pharmacogenetics and model-informed precision dosing to improve patient care. *Br. J. Clin. Pharmacol.* (2020).doi:https://doi.org/10.1111/bcp.14426

42. Vinks, A. A. *et al.* Electronic Health Record–Embedded Decision Support Platform for Morphine Precision Dosing in Neonates. *Clin. Pharmacol. Ther.* **107**, 186–194 (2020).

Table 1. Study Cohort

Summary of demographic, genotype, clinical, dosing, and specimen sampling characteristics

	Entire cohort
n	354
Postnatal Age (months)	15.7 (5.3 – 61.8) [0.03, 270.9]
Postmenstrual Age (weeks)	104.6 (61.7 – 303.7) [39.1, 1200.0]
Median weight (kg)	9.4 (6.0 – 18.2) [2.0, 138.0]
Male sex	183 (52%)
Race	
White	293 (83%)
Black	40 (11%)
American Indian or Alaska Native	2 (1%)
Asian	6 (2%)
Other	5 (1%)
Unknown	8 (2%)
Median serum creatinine (mg/dL)	0.49 (0.44 – 0.56) [0.24, 1.12]
STAT score	
1	154 (43%)
2	108 (31%)
3	41 (12%)
4	46 (13%)
5	5 (1%)
UGT1A4 variants	
0	262 (74%)
1	87 (25%)
2	5 (1%)
UGT2B10 variants	
0	186 (53%)
1	117 (33%)
2 or 3	51 (14%)
CYP2A6 score [a]	2.04 (2.00 – 2.21) [1.58, 2.43]
Cardiac bypass time (hr)	1.66 (1.2 – 2.4) [0, 7.1]
Length of ICU hospitalization (days)	4 (2 – 6) [1, 120]
Total dosing events [b]	2386

Total IV infusion doses	2351
Infusion duration (hr)	2.0 (1.0 – 5.1) [0.02, 125.6]
Infusion rate (mcg/kg/hr)	0.6 (0.5 – 1.0) [0.03, 2.0]
Total IV bolus doses	35
Bolus dose amount (mcg/kg)	1.00 (0.96 – 1.01) [0.06, 4.21]
Dosing events per subject	5 (3 – 8) [1, 37]
Total dexmedetomidine concentration measurements	1400
Dexmedetomidine measurements below lower limit of quantification	120
Dexmedetomidine measurements per subject	3 (2 – 5) [1, 18]
First dexmedetomidine measurement time after dose start (hr)	5.3 (3.7 – 11.3) [0, 178.5]
Final dexmedetomidine measurement time after dose start (hr)	67.7 (39.3 – 130.5) [2.0, 659.8]

Continuous variable summary statistics: median (interquartile range) [minimum, maximum]; Categorical variable summary statistics: number (%); [a]Among n=350 subjects with available score; [b] A dosing event is defined as a bolus administration or an infusion interval with constant administration rate for a specific duration.

Table 2. Estimates of Parameters for Population Pharmacokinetic Models

(A) Estimates from base model and covariate models without genetic covariates. Weight is modeled with fixed allometric scaling parameters.

Base Model (Obj = -1517.3; BICc = -1415.1)		**Weight Only Model** (Obj = -1923.3; BICc = -1821.1)		**Weight and Maturation with simplified variance structure** (Obj = -1915.1; BICc = -1835.0)	
Parameters	Estimates (SE) [95% CI][a]	Parameters	Estimates (SE) [95% CI]	Parameters	Estimates (SE) [95% CI]
CL		$CL = \theta_1(WT/70)^{0.75}$		$CL = \theta_1(WT/70)^{0.75}\left(\frac{1}{1+\left(\frac{TM_{50}}{PMA}\right)^{Hill}}\right)$	
	6.27 (0.52) [5.33, 7.37]	θ_1	22.3 (1.85) [19.0, 26.2]	θ_1	27.3 (1.82) [24.0, 31.1]
				TM_{50}	41.9 (0.28) [41.4, 42.5]
				Hill	7.04 (0.022) [6.99, 7.08]
V_1		$V_1 = \theta_2(WT/70)$		$V_1 = \theta_2(WT/70)$	
	19.5 (1.37) [17.0, 22.4]	θ_2	123 (11.5) [102, 148]	θ_2	161 (12.1) [139, 187]
Q		$Q = \theta_3(WT/70)^{0.75}$		$Q = \theta_3(WT/70)^{0.75}$	
	5.26 (0.44) [4.47, 6.20]	θ_3	26.6 (2.23) [22.6, 31.3]	θ_3	26.0 (1.90) [22.5, 30.0]
V_2		$V_2 = \theta_4(WT/70)$		$V_2 = \theta_4(WT/70)$	
	763 (126) [555, 1048]	θ_4	6674 (1499) [4363, 10211]	θ_4	7903 (1408) [5617, 11119]
ω_{CL} (%CV)	201 (12) [178, 226]	ω_{CL} (%CV)	123 (13) [100, 150]	ω_{CL} (%CV)	103 (8) [88, 120]
ω_{V1} (%CV)	161 (9) [145, 179]	ω_{V1} (%CV)	168 (22) [130, 217]	ω_{V1} (%CV)	138 (13) [114, 166]
ω_{Q} (%CV)	146 (8) [132, 162]	ω_{Q} (%CV)	91 (11) [71, 115]	ω_{Q} (%CV)	82 (9) [65, 102]
ω_{V2} (%CV)	672 (81) [534, 855]	ω_{V2} (%CV)	857 (256) [494, 1595]	ω_{V2} (%CV)	624 (157) [391, 1048]

Base Model (Obj = -1517.3; BICc = -1415.1)		**Weight Only Model** (Obj = -1923.3; BICc = -1821.1)		**Weight and Maturation with simplified variance structure** (Obj = -1915.1; BICc = -1835.0)	
$\rho_{CL,V1}$	0.964 (0.003) [0.959, 0.97]	$\rho_{CL,V1}$	0.849 (0.055) [0.741, 0.956]	$\rho_{CL,V1}$	0.923 (0.027) [0.871, 0.975]
$\rho_{CL,V2}$	-0.032 (0.043) [-0.116, 0.053]	$\rho_{CL,V2}$	-0.174 (0.101) [-0.372, 0.023]	$\rho_{CL,V2}$	0 (fixed)
$\rho_{CL,Q}$	0.043 (0.076) [-0.106, 0.192]	$\rho_{CL,Q}$	-0.509 (0.110) [-0.726, -0.293]	$\rho_{CL,Q}$	0 (fixed)
$\rho_{V1,V2}$	0.195 (0.044) [0.109, 0.28]	$\rho_{V1,V2}$	0.277 (0.107) [0.068, 0.486]	$\rho_{V1,V2}$	0 (fixed)
$\rho_{V1,Q}$	-0.076 (0.073) [-0.22, 0.067]	$\rho_{V1,Q}$	-0.410 (0.125) [-0.656, -0.165]	$\rho_{V1,Q}$	0 (fixed)
$\rho_{V2,Q}$	0.089 (0.083) [-0.074, 0.252]	$\rho_{V2,Q}$	0.21 (0.121) [-0.028, 0.448]	$\rho_{V2,Q}$	0 (fixed)
σ_{add} (ng/mL)	2.22e-16 (5.65e-13) [0, 1.11e-12]	σ_{add} (ng/mL)	1.9e-08 (3.73e-07) [0, 7.51e-07]	σ_{add} (ng/mL)	0 (fixed)
σ_{prop} (%CV)	50.3 (1.4) [47.6, 53.0]	σ_{prop} (%CV)	50.3 (1.6) [47.2, 53.4]	σ_{prop} (%CV)	50.5 (1.6) [47.5, 53.5]

(B) Estimates from categorical gene models for *UGT1A4* or *UGT2B10*.

***UGT1A4* Categorical Gene Model** (Obj = -1918.3; BICc = -1832.4)		***UGT2B10* Categorical Gene Model** (Obj = -1913.8; BICc = -1827.9)	
Parameters	Estimates (SE) [95% CI]	Parameters	Estimates (SE) [95% CI]
$CL = \theta_1(WT/70)^{0.75}\left(\frac{1}{1+\left(\frac{TM_{50}}{PMA}\right)^{Hill}}\right)\exp(\theta_5 I[UGT1A4 > 0])$		$CL = \theta_1(WT/70)^{0.75}\left(\frac{1}{1+\left(\frac{TM_{50}}{PMA}\right)^{Hill}}\right)\exp(\theta_5 I[UGT2B10 > 0])$	
θ_1	24.0 (2.19) [20.1, 28.7]	θ_1	20.4 (2.07) [16.8, 24.9]
TM_{50}	42.2 (0.041) [42.1, 42.3]	TM_{50}	45.7 (0.078) [45.6, 45.9]
Hill	4.17 (0.0016) [4.16, 4.17]	Hill	4.96 (0.0073) [4.95, 4.97]
θ_5	-0.221 (0.16) [-0.54, 0.09]	θ_5	-0.104 (0.11) [-0.32, 0.11]
$V_1 = \theta_2(WT/70)$		$V_1 = \theta_2(WT/70)$	
θ_2	169 (20.4) [133, 213]	θ_2	178 (12.6) [155, 204]
$Q = \theta_3(WT/70)^{0.75}$		$Q = \theta_3(WT/70)^{0.75}$	
θ_3	31.2 (2.74) [26.3, 37.1]	θ_3	33.2 (1.84) [29.8, 37.0]
$V_2 = \theta_4(WT/70)$		$V_2 = \theta_4(WT/70)$	
θ_4	14346 (2782) [9908, 20770]	θ_4	19655 (2804) [14921, 25889]
ω_{CL} (%CV)	113 (13) [90, 140]	ω_{CL} (%CV)	131 (13) [108, 158]
ω_{V1} (%CV)	139 (31) [88, 216]	ω_{V1} (%CV)	126 (12) [104, 152]

***UGT1A4* Categorical Gene Model** (Obj = -1918.3; BICc = -1832.4)		***UGT2B10* Categorical Gene Model** (Obj = -1913.8; BICc = -1827.9)	
ω_Q (%CV)	67 (7) [54, 81]	ω_Q (%CV)	67 (6) [56, 79]
ω_{V2} (%CV)	640 (158) [404, 1067]	ω_{V2} (%CV)	544 (114) [367, 837]
$\rho_{CL,V1}$	0.953 (0.043) [0.869, 1.0]	$\rho_{CL,V1}$	0.939 (0.018) [0.904, 0.974]
$\rho_{CL,V2}$	0 (fixed)	$\rho_{CL,V2}$	0 (fixed)
$\rho_{CL,Q}$	0 (fixed)	$\rho_{CL,Q}$	0 (fixed)
$\rho_{V1,V2}$	0 (fixed)	$\rho_{V1,V2}$	0 (fixed)
$\rho_{V1,Q}$	0 (fixed)	$\rho_{V1,Q}$	0 (fixed)
$\rho_{V2,Q}$	0 (fixed)	$\rho_{V2,Q}$	0 (fixed)
σ_{add} (ng/mL)	0 (fixed)	σ_{add} (ng/mL)	0 (fixed)
σ_{prop} (%CV)	50.6 (1.6) [47.5, 53.8]	σ_{prop} (%CV)	50.7 (1.6) [47.6, 53.8]

(C) Estimates from additive gene models for *UGT1A4* or *UGT2B10*.

***UGT1A4* Additive Gene Model** (Obj = -1917.6; BICc = -1831.7)		***UGT2B10* Additive Gene Model** (Obj = -1917.3; BICc = -1831.4)	
Parameters	Estimates (SE) [95% CI]	Parameters	Estimates (SE) [95% CI]
$CL = \theta_1(WT/70)^{0.75}\left(\frac{1}{1+\left(\frac{TM_{50}}{PMA}\right)^{Hill}}\right)\exp(\theta_5 UGT1A4)$		$CL = \theta_1(WT/70)^{0.75}\left(\frac{1}{1+\left(\frac{TM_{50}}{PMA}\right)^{Hill}}\right)\exp(\theta_5 UGT2B10)$	
θ_1	23.8 (2.47) [19.5, 29.1]	θ_1	23.5 (2.43) [19.2, 28.7]
TM_{50}	47.6 (0.136) [47.3, 47.9]	TM_{50}	41.6 (0.206) [41.2, 42.0]
Hill	5.55 (0.013) [5.53, 5.58]	Hill	17.6 (0.052) [17.5, 17.7]
θ_5	-0.166 (0.12) [-0.406, 0.073]	θ_5	-0.108 (0.068) [-0.241, 0.025]
$V_1 = \theta_2(WT/70)$		$V_1 = \theta_2(WT/70)$	
θ_2	171 (16.2) [142, 206]	θ_2	161 (14.2) [136, 191]
$Q = \theta_3(WT/70)^{0.75}$		$Q = \theta_3(WT/70)^{0.75}$	
θ_3	31.6 (2.1) [27.7, 36.0]	θ_3	31.5 (2.2) [27.5, 36.0]
$V_2 = \theta_4(WT/70)$		$V_2 = \theta_4(WT/70)$	
θ_4	16576 (3229) [11431, 24038]	θ_4	12588 (2603) [8495, 18654]
ω_{CL} (%CV)	110 (10) [91, 131]	ω_{CL} (%CV)	109 (12) [88, 135]
ω_{V1} (%CV)	136 (18) [104, 177]	ω_{V1} (%CV)	139 (14) [113, 170]

***UGT1A4* Additive Gene Model** (Obj = -1917.6; BICc = -1831.7)		***UGT2B10* Additive Gene Model** (Obj = -1917.3; BICc = -1831.4)	
ω_Q (%CV)	69 (7) [56, 84]	ω_Q (%CV)	64 (7) [52, 78]
ω_{V2} (%CV)	548 (120) [364, 858]	ω_{V2} (%CV)	792 (212) [482, 1377]
$\rho_{CL,V1}$	0.933 (0.03) [0.88, 0.99]	$\rho_{CL,V1}$	0.943 (0.04) [0.87, 1.0]
$\rho_{CL,V2}$	0 (fixed)	$\rho_{CL,V2}$	0 (fixed)
$\rho_{CL,Q}$	0 (fixed)	$\rho_{CL,Q}$	0 (fixed)
$\rho_{V1,V2}$	0 (fixed)	$\rho_{V1,V2}$	0 (fixed)
$\rho_{V1,Q}$	0 (fixed)	$\rho_{V1,Q}$	0 (fixed)
$\rho_{V2,Q}$	0 (fixed)	$\rho_{V2,Q}$	0 (fixed)
σ_{add} (ng/mL)	0 (fixed)	σ_{add} (ng/mL)	0 (fixed)
σ_{prop} (%CV)	50.4 (1.6) [47.4, 53.5]	σ_{prop} (%CV)	50.6 (1.6) [47.5, 53.7]

(D) Estimates from models using weight and maturation with simplified variance structure in *CYP2A6* PRS subset.

Without *CYP2A6* Score (Obj = -1889.2; BICc = -1809.3)		**With *CYP2A6* Score** (Obj = -1889.9; BICc = -1804.2)	
Parameters	Estimates (SE) [95% CI]	Parameters	Estimates (SE) [95% CI]
$CL = \theta_1(WT/70)^{0.75}\left(\frac{1}{1+\left(\frac{TM_{50}}{PMA}\right)^{Hill}}\right)$		$CL = \theta_1(WT/70)^{0.75}\left(\frac{1}{1+\left(\frac{TM_{50}}{PMA}\right)^{Hill}}\right)\exp\left(\theta_5(CY2A6score)\right)$	
θ_1	30.5 (2.16) [26.5, 35.0]	θ_1	24.8 (14.7) [9.42, 65.2]
TM_{50}	41.5 (0.046) [41.4, 41.6]	TM_{50}	42.6 (0.098) [42.4, 42.8]
Hill	4.52 (0.011) [4.50, 4.54]	Hill	7.45 (0.015) [7.42, 7.48]
		θ_5	0.0885 (0.28) [-0.46, 0.64]
$V_1 = \theta_2(WT/70)$		$V_1 = \theta_2(WT/70)$	
θ_2	157 (16.1) [128, 191]	θ_2	152 (12.1) [130, 178]
$Q = \theta_3(WT/70)^{0.75}$		$Q = \theta_3(WT/70)^{0.75}$	
θ_3	24.8 (1.99) [21.2, 29.0]	θ_3	24.5 (1.78) [21.2, 28.2]
$V_2 = \theta_4(WT/70)$		$V_2 = \theta_4(WT/70)$	
θ_4	5720 (1129) [3925, 8335]	θ_4	5756 (1017) [4102, 8077]
ω_{CL} (%CV)	103 (10) [86, 124]	ω_{CL} (%CV)	100 (8) [86, 116]
ω_{V1} (%CV)	129 (20) [95, 173]	ω_{V1} (%CV)	138 (15) [111, 171]

Without *CYP2A6* Score (Obj = -1889.2; BICc = -1809.3)		**With *CYP2A6* Score** (Obj = -1889.9; BICc = -1804.2)	
ω_Q (%CV)	87 (10) [69, 109]	ω_Q (%CV)	86 (9) [69, 106]
ω_{V2} (%CV)	514 (118) [334, 825]	ω_{V2} (%CV)	549 (133) [349, 906]
$\rho_{CL,V1}$	0.945 (0.03) [0.88, 1.0]	$\rho_{CL,V1}$	0.942 (0.02) [0.91, 0.98]
$\rho_{CL,V2}$	0 (fixed)	$\rho_{CL,V2}$	0 (fixed)
$\rho_{CL,Q}$	0 (fixed)	$\rho_{CL,Q}$	0 (fixed)
$\rho_{V1,V2}$	0 (fixed)	$\rho_{V1,V2}$	0 (fixed)
$\rho_{V1,Q}$	0 (fixed)	$\rho_{V1,Q}$	0 (fixed)
$\rho_{V2,Q}$	0 (fixed)	$\rho_{V2,Q}$	0 (fixed)
σ_{add} (ng/mL)	0 (fixed)	σ_{add} (ng/mL)	0 (fixed)
σ_{prop} (%CV)	50.8 (1.6) [47.6, 54.0]	σ_{prop} (%CV)	50.7 (1.6) [47.7, 53.8]

Abbreviations: [a] 95% Asymptotic confidence intervals (CIs); SE, standard error; Obj, objective function value; BICc, corrected Bayesian information criteria; CL, total clearance (L/hr); Q, intercompartmental clearance (L/hr); V_1, volume of distribution for the central compartment (L); V_2, volume of distribution for the peripheral compartment (L); TM_{50} postmenstrual age at which clearance is 50% of adult value; Hill, maturation factor slope coefficient; CV, coefficient of variation; WT, body weight in kg; PMA, postmenstrual age in weeks; ω_{CL}, ω_{V1}, ω_Q, ω_{V2}, the standard deviation for η_i^{CL}, η_i^{V1}, η_i^Q, and η_i^{V2}, respectively; For the standard deviation of random effects, ω, coefficient of variation was calculated as CV% = $100 \times \sqrt{(exp(\omega^2) - 1)}$; ρ are correlation terms between random effects; σ_{prop} and σ_{add} are proportional and additive residual error terms.

Figure 1. Study Cohort Flow Diagram in Data Processing with Exclusion Criteria

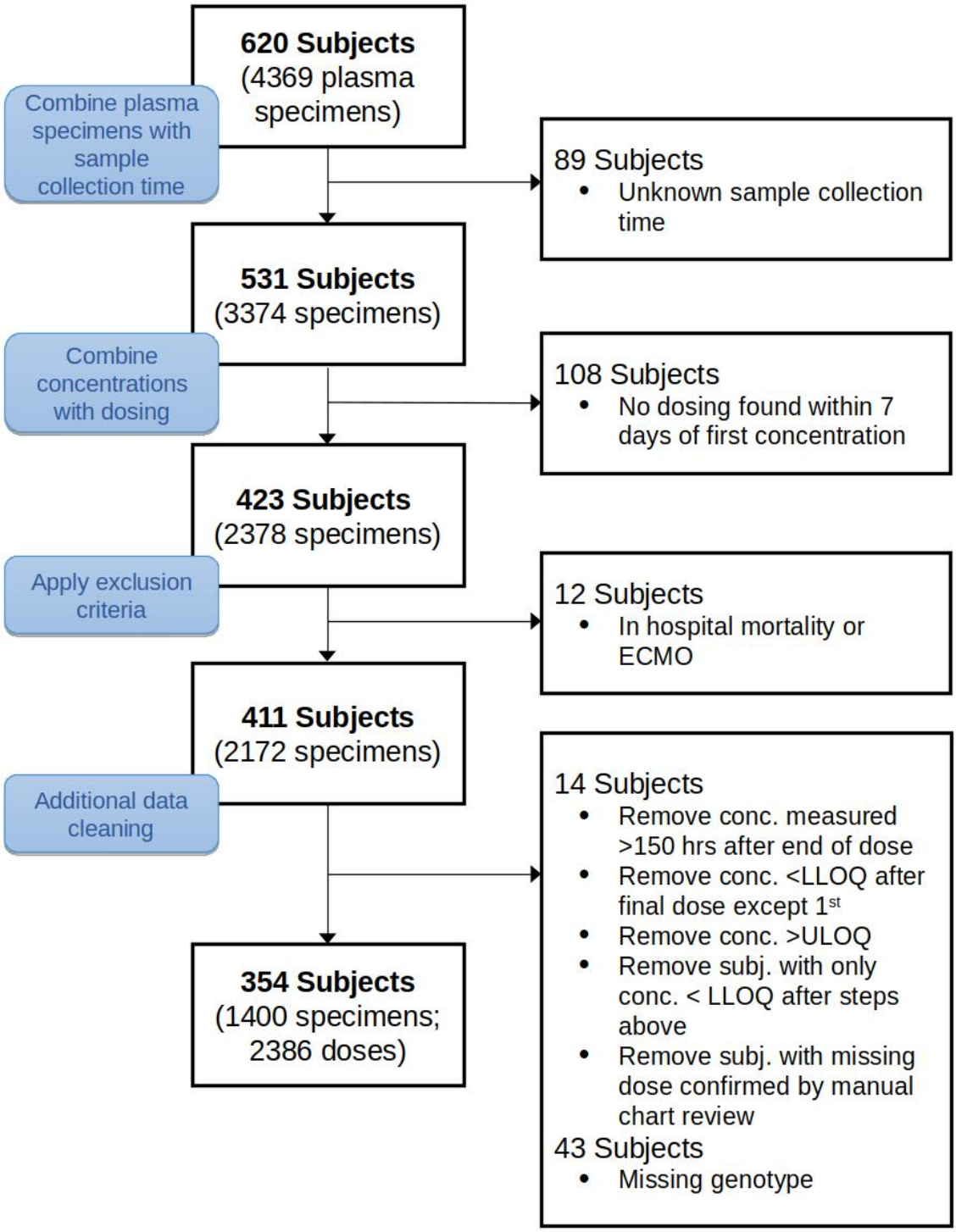

Figure 2. Diagnostic plots for the final population PK model

(A) Observed dexmedetomidine concentrations vs. population predicted and (B) individual predicted concentrations. Filled circles indicate observed values, "x"s indicate simulated values based on the estimated model for observations below the lower limit of quantification (0.005 ng/mL), blue lines are loess smoothers, and the solid black lines represent the line of identity

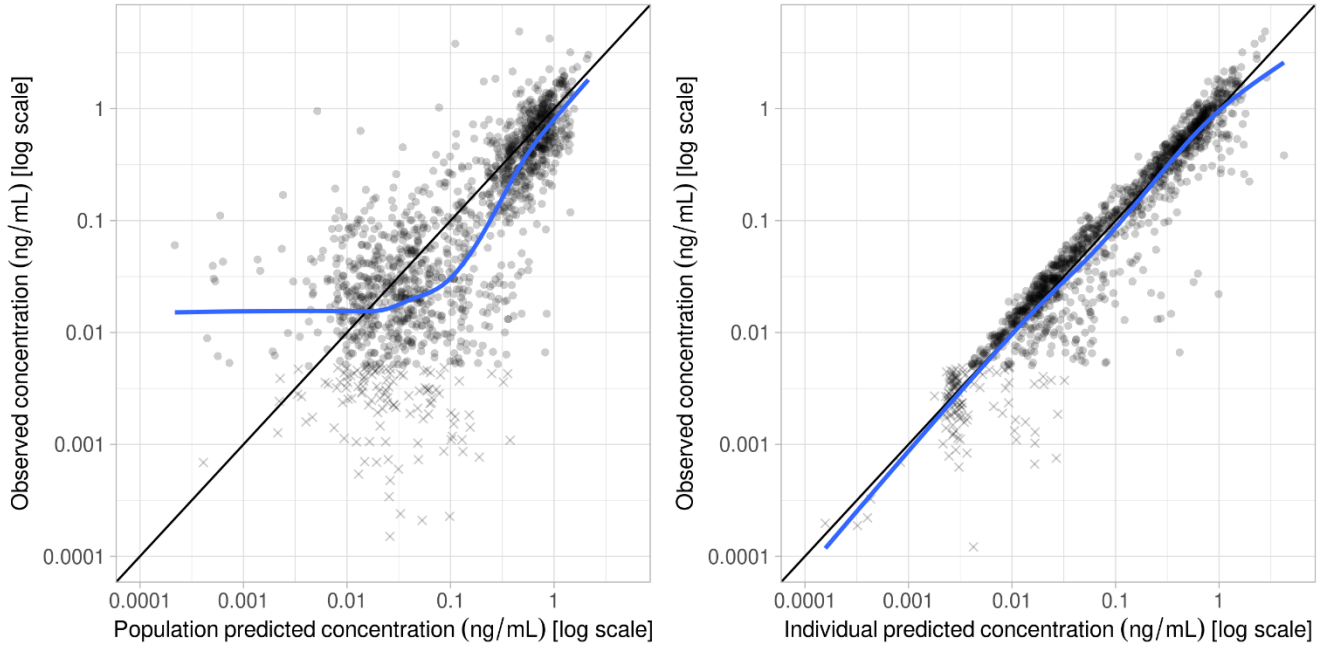

(C) Individual weighted residuals vs. predicted concentrations and (D) time. Blue lines are loess smoothers, and the black horizontal lines at zero represent no trend

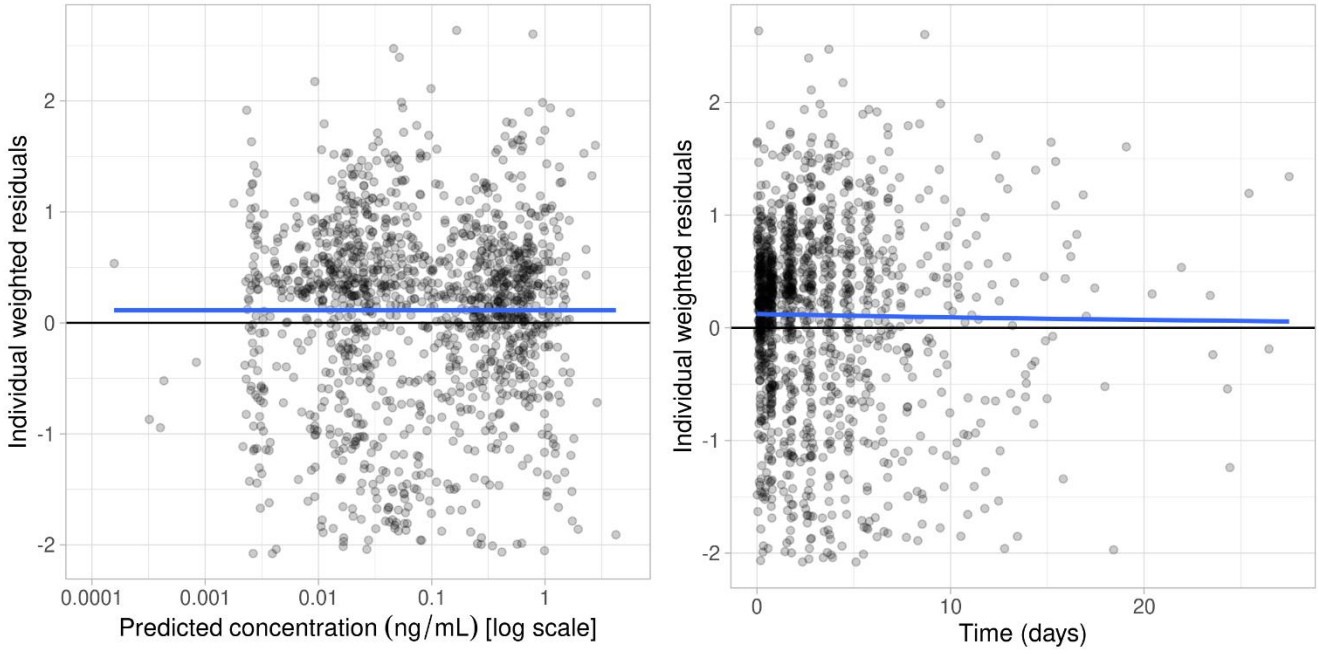

(E) Correlation between random effects. Blue lines are least-squares fits

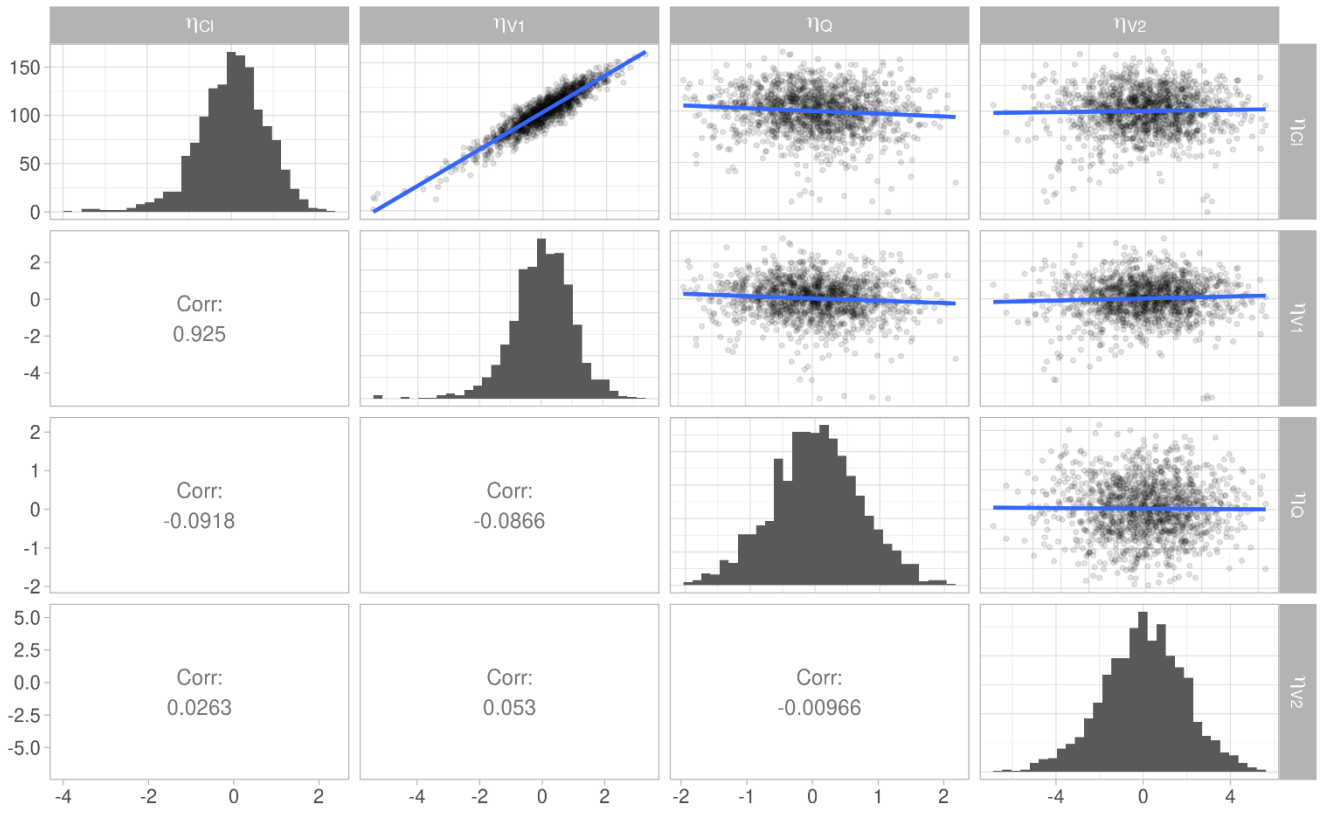

(F) Random effects vs. continuous and (G) categorical covariates. Blue lines are loess smoothers

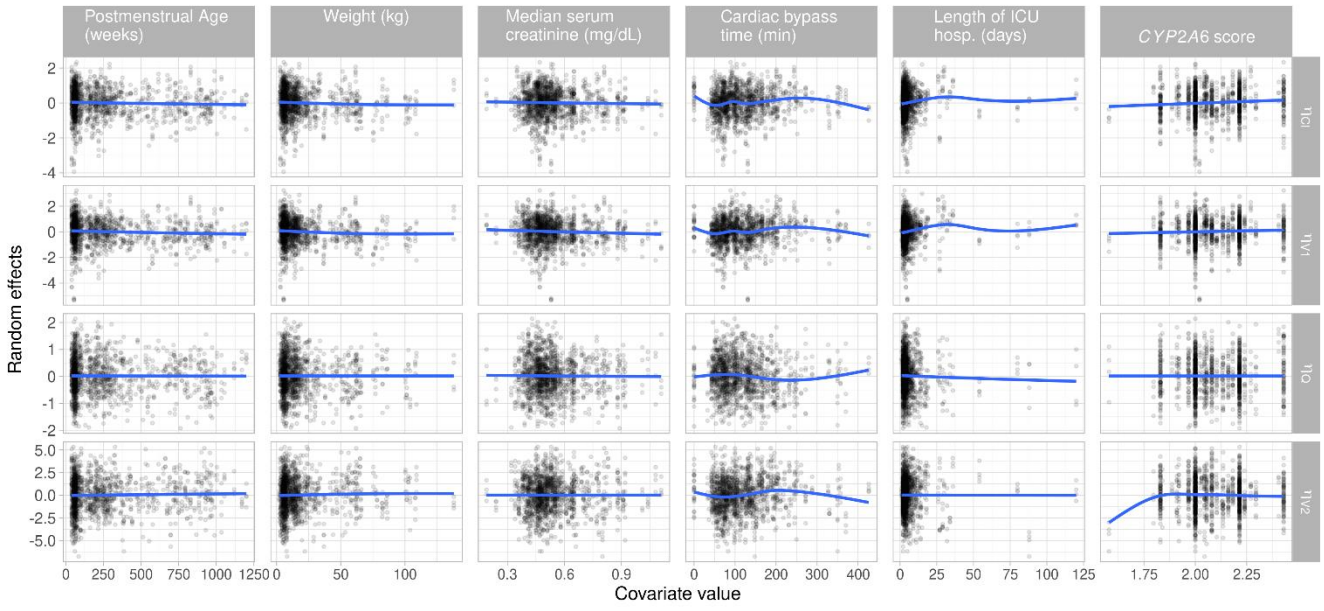

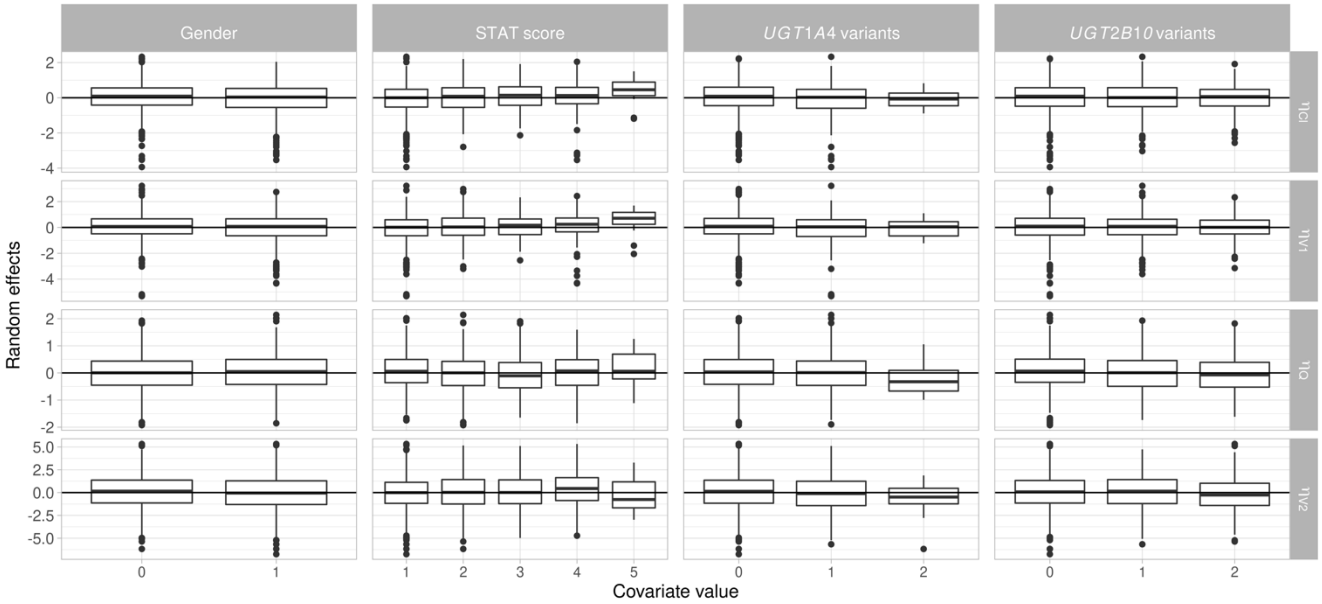

(H) Prediction-corrected visual predictive check with 10th, 50th and 90th percentile of observed values (solid lines) and theoretical values (dashed lines) along with 90% prediction interval for theoretical percentiles (shaded region). Filled circles indicate observed values, "x"s indicate simulated values based on the estimated model for observations below the lower limit of quantification of 0.005 ng/mL (represented by a horizontal gray line); time was binned using the least-squares criteria.

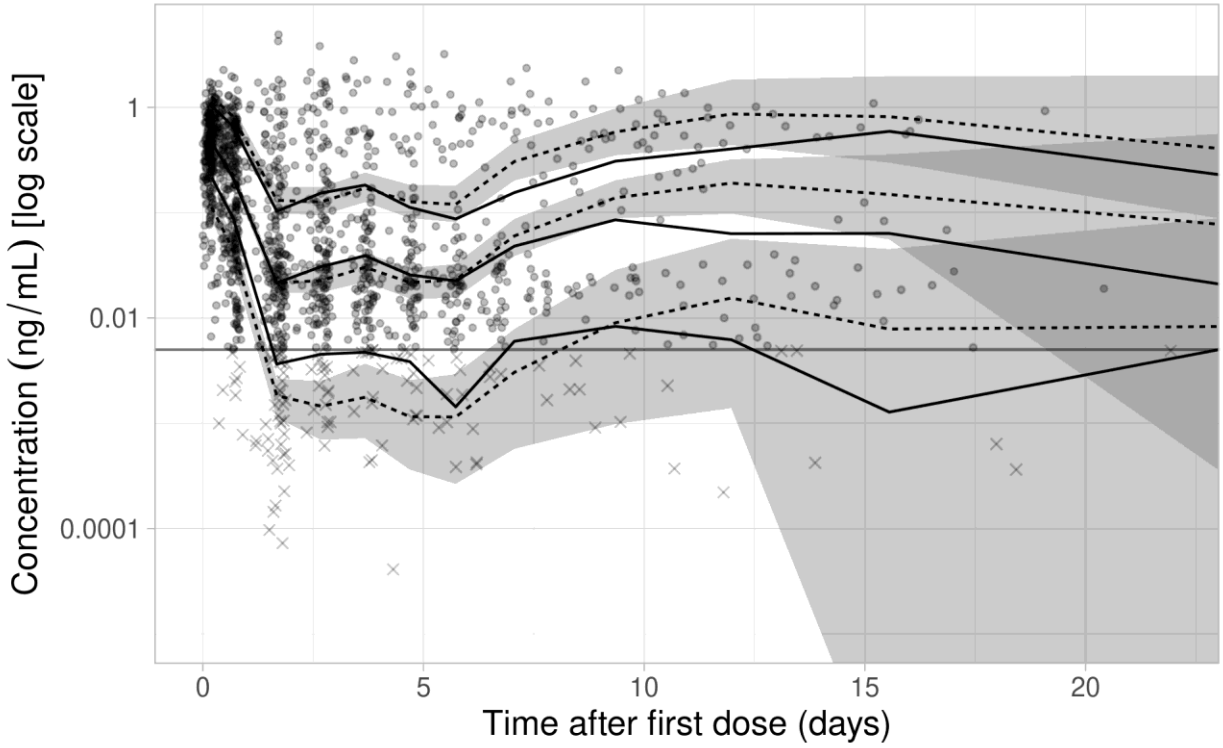

Figure 3. Predicted clearance by weight for selected ages from the final weight and age maturation model

Plausible weight ranges for each age group are: 41 weeks (2.7 to 5.1 kg), 45 weeks (3.3 to 6.1 kg), 53 weeks (4.5 to 8.0 kg), 69 weeks (6.3 to 10.8 kg), 93 weeks (8.1 to 13.4 kg), 117 weeks (9.3 to 14.9 kg), 183 weeks (11.2 to 18.1 kg). Overlapping lines between different age categories represent weights that are plausible for multiple age groups.